

Provided for non-commercial research and education use.  
Not for reproduction, distribution or commercial use.



This article appeared in a journal published by Elsevier. The attached copy is furnished to the author for internal non-commercial research and education use, including for instruction at the authors institution and sharing with colleagues.

Other uses, including reproduction and distribution, or selling or licensing copies, or posting to personal, institutional or third party websites are prohibited.

In most cases authors are permitted to post their version of the article (e.g. in Word or Tex form) to their personal website or institutional repository. Authors requiring further information regarding Elsevier's archiving and manuscript policies are encouraged to visit:

<http://www.elsevier.com/copyright>



Contents lists available at ScienceDirect

Tetrahedron

journal homepage: [www.elsevier.com/locate/tet](http://www.elsevier.com/locate/tet)

## Synthesis and solid-state dynamics of molecular dirotors

Stephanie L. Gould, Richard B. Rodriguez, Miguel A. Garcia-Garibay\*

Department of Chemistry and Biochemistry, University of California, Los Angeles, CA 90095-1569, USA

### ARTICLE INFO

#### Article history:

Received 14 March 2008

Received in revised form 15 May 2008

Accepted 30 May 2008

Available online 6 June 2008

### ABSTRACT

We report the design, synthesis, thermal properties, and dynamic NMR characterization of four new molecular dirotors, each containing two rotary 1,4-diethynyl phenylene units, a bridging 1,3-bis(diphenylmethyl) benzene stator, and two capping triphenylmethyl groups. These compounds are variations of the well-known wheel and axle structures. Ambient temperature quadrupolar echo  $^2\text{H}$  NMR spectra of phenylene-deuterated samples revealed line shapes consistent with dynamic processes having exchange rates  $>10^8 \text{ s}^{-1}$ , and more than the two minima typically observed for most phenylene rotators. Reasonable line-shape simulations were obtained with a model that involves four minima related by angular displacements of  $0^\circ$ ,  $30^\circ$ ,  $180^\circ$ , and  $230^\circ$ . Cooling the samples to 260 K revealed spectra consistent with samples that contain two or more components. These results indicate that novel wheel and axle structures do create a certain amount of free volume that allows for the desired mobility of the rotating units.

© 2008 Elsevier Ltd. All rights reserved.

### 1. Introduction

Most recent progress in the field of artificial molecular machinery has been based on the design and testing of functional molecules in solution.<sup>1–3</sup> Recognizing that macroscopic and biological machineries are part of complex assemblies with a well-defined and external frame of reference, recent efforts in the community have shifted toward the construction of artificial molecular machinery supported on surfaces<sup>4–6</sup> and three-dimensional crystalline aggregates.<sup>7–9</sup> To describe the coexistence of rigid and mobile elements in ordered arrays we recently suggested the term ‘amphidynamic crystals’.<sup>10,11</sup> With hopes of emulating machines in the macroscopic and biomolecular realms, we suggested that amphidynamic materials could be built with structural designs based on: (a) free volume compartments, (b) volume-conserving motions, such as the rotation of a cylinder along its principal axis, and/or (c) the concerted motions of two or more components.

Our initial ventures into molecular machinery focused on the design and study of crystals built with molecules that mimic some elements of macroscopic gyroscopes (Fig. 1). These compounds have a phenylene rotator with a virtually barrierless dialkyne linkage<sup>12</sup> (shown in red), and two bulky triarylmethyl<sup>13–15</sup> (or triptycyl)<sup>16</sup> groups that provide steric shielding and define a static frame of reference in the crystal (shown in blue). Using variable temperature solid-state NMR spectroscopy,<sup>13–16</sup> X-ray thermal

anisotropic parameters,<sup>17</sup> force-field models,<sup>18</sup> and dielectric spectroscopy with fluorinated analogs,<sup>19,20</sup> we have shown that the internal dynamics of molecular gyroscopes with phenylene rotators depend on the structure of the stator.<sup>10,11</sup> Crystalline solids with

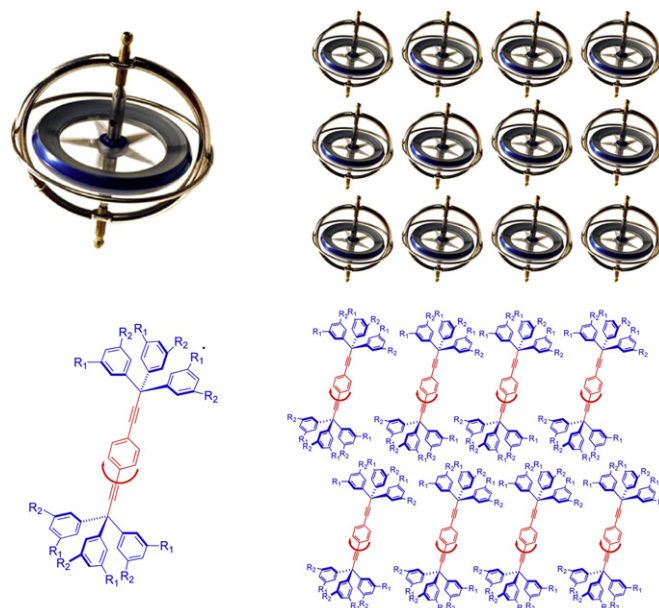


**Figure 1.** An illustration of a macroscopic toy gyroscope (top), and molecular gyroscopes with a single rotator having open (bottom) topology.

\* Corresponding author. Tel.: +1 310 825 3159; fax: +1 310 825 0767.  
E-mail address: [mgg@chem.ucla.edu](mailto:mgg@chem.ucla.edu) (M.A. Garcia-Garibay).

molecular gyroscopes having various triarylmethyl (trityl) stators showed ambient temperature rotational frequencies varying from ca.  $10^3 \text{ s}^{-1}$  (Fig. 1,  $R_1=R_2=H$ ) to ca.  $10^9 \text{ s}^{-1}$  ( $R_1=R_2=t\text{-Bu}$ ). Their packing properties are consistent with those of molecules with a long and rigid rod capped with bulky ends. With shapes that resemble a *wheel* and an *axle*, these molecules, are known to form relatively low-density crystals with a tendency to trap solvent of crystallization.<sup>21,22</sup>

Analyzing *wheel and axle* structures, Soldatov<sup>22</sup> recently noted that in addition to structures with two bulky ends linked by a rigid rod,<sup>23–25</sup> low-density crystals are also formed by structures with shapes that consist of rigid platforms penetrated by a rod,<sup>1d,26,27</sup> or several platforms penetrated or interconnected by one or more rods.<sup>28,29</sup> The common feature of these structural motifs is that close packing structures with complementary contact for all their surfaces are impossible, so that they tend to require solvent of crystallization.<sup>30</sup>

Recognizing that these low-density structures may be conducive to various types of amphidynamic materials, and with the goal of increasing the structural and dynamic complexities of potential molecular machinery components, we decided to investigate the synthesis and characterization of several types of covalently linked molecular rotors. As illustrated in Figure 2, several topologies and rotor connectivities may be envisioned with stators represented in

blue and rotators in red. Among them are structures with two stators and several internal rotators in the same rotary axle (Fig. 2b), structures with two (or more) rotators sharing a common central stator (Fig. 2c), and cyclic structures with two or more stators that are either covalently linked (Fig. 2d), or shared (Fig. 2e). Notably, multirotor connectivities such as that illustrated in Figure 2d can be extended in extended 3D dimensional lattices by taking advantage of metal organic frameworks (MOFs).<sup>31</sup>

The realization of structures corresponding to Figure 2b–e represents an interesting synthetic challenge and pose several questions regarding the crystallization and dynamics of molecules with multiple rotators. Since phenylene librations and internal rotations are the result of coupled vibrations along the rotary axis and the local environment, it will be interesting to identify the structural attributes that may cause different rotators to have the same or different frequencies, and whether they can act independent of each other, or are correlated. As a first step to answer these and other questions we decided to start with the structures based on structural elements previously studied in our group such as trityl and triptycyl stators, and diethynyl phenylene rotators (Fig. 2). Structure I is based on a central 1,3-bis(diphenylmethyl)benzene stator that permits changes in orientation of the two rotors that may explore to form cyclic structures such that in Fig. 2d. Structures II and III are based on a central triptycene that maintains

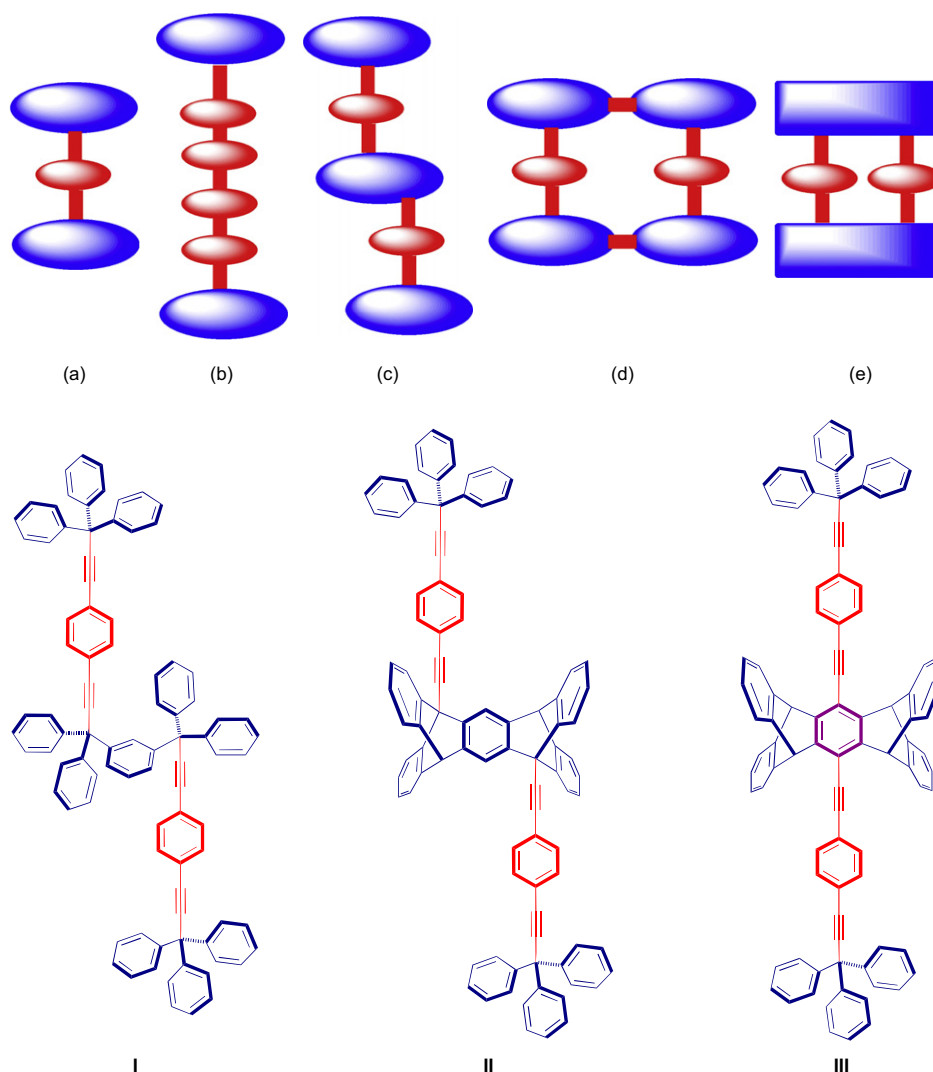


**Figure 2.** (Top) Schematic representation of multirotor structures expected to have low packing density and rapid rotary dynamics. (Bottom) Potential dirotor structures analogous to (c), with trityl and triptycyl groups as stators and phenylene groups as rotators.

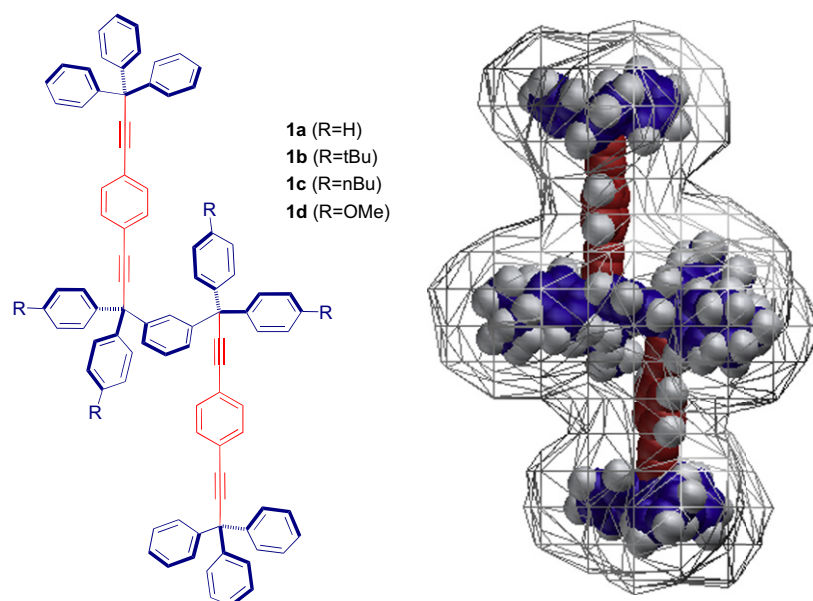


**Figure 3.** Line formula of dirotor **1**, with two phenylene rotators sharing a bistrityl stator, and a corresponding space filling model with a 4 Å van der Waals surface.

the two rotators in a rigid and opposite orientation. With the two rotators linked at the  $sp^2$  carbons of the central pentiptycene ring, structure III maintains the two rotators co-linear and conjugated. As a first step to explore the synthesis and physical properties of these structures we decide to start with compounds **1a–1d**, which are representative of structure I (Fig. 3). By linking the two rotators with a bridging stator we hope to take advantage of synthetic strategies recently developed in our group. Based on space filling models, we expected the modified 1,3-bis(diphenylmethyl) group at the center of the structure to provide the rotators with a large amount of free volume, which should be manifested as a very fast rotation. While the single rotators studied previously (molecular gyroscopes) were found to interdigitate upon crystallization, the central platform of compound **1** has the potential of preventing adjacent molecules from occupying the space surrounding their central phenylene.

We report here the synthesis and characterization of natural abundance and the phenylene- $d_4$  derivative of the unsubstituted compound (**1a**), as well as three derivatives with *para-tert*-butyl (**1b**), *para-n*-butyl (**1c**), and *para*-methoxy (**1d**) groups attached to the bridging stator. While we have been unable to obtain single crystals for X-ray diffraction characterization, we have established that they have significantly faster rotary dynamics than analogous monorotors.

## 2. Results and discussion

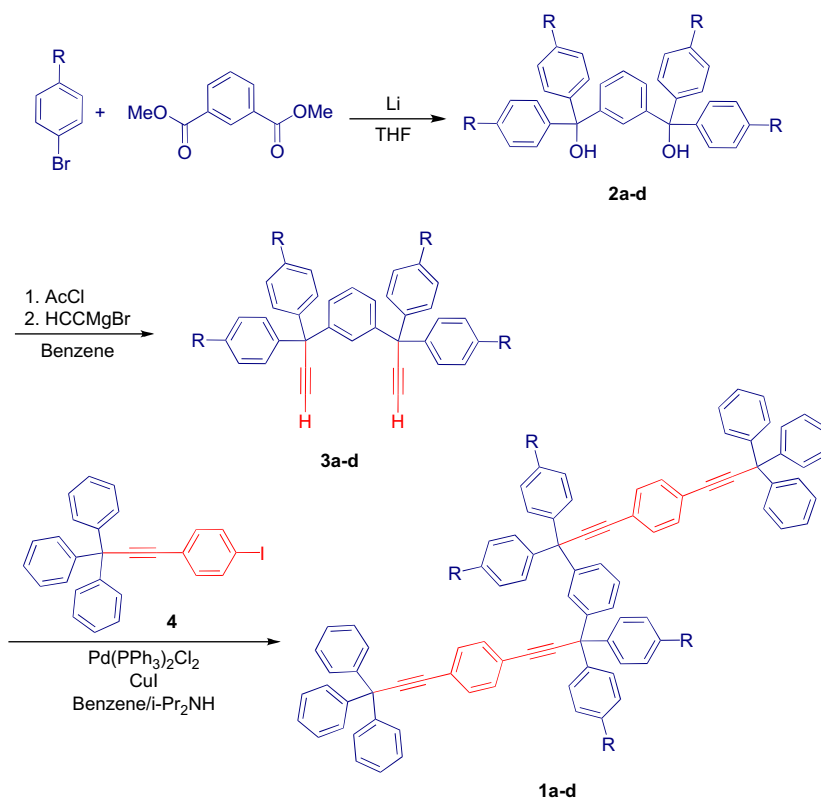
### 2.1. Synthesis and characterization

Molecular dirotors **1a–1d** were synthesized by a convergent synthesis centered on a double coupling reaction analogous to the one used for preparation of the single rotor ‘gyroscopes’ (Scheme 1).<sup>14</sup> A *para*-substituted bromobenzene was reacted with lithium metal to form the corresponding anion, which was subsequently reacted with dimethyl isophthalate to form diols **2a–2c** in isolated yields of ca. 40%. The methoxy diol **2d** was obtained in similar manner in 62% yield. Dialkynyl compounds **3a–3d** were obtained by reaction of **2a–2d** with acetyl chloride followed by a substitution reaction with ethynyl magnesium bromide in refluxing benzene. The unsubstituted dialkyne **3a** and the methoxy derivative **3d**, formed in 52% and 41% yields, respectively.

Significantly higher yields were obtained for the *tert*-butyl (**3b**) and *n*-butyl compounds (**3c**) (83% and 61% yields, respectively). The required 4-(3',3',3'-triphenylpropynyl)-1-iodobenzene (**4**) was prepared by the literature procedures<sup>32</sup> and submitted to the final coupling reaction with **3a–3d** to give dirotors **1a–1d** in approximately 50% yield. The solubility of each compound varied considerably. Unsubstituted dirotor **1a** was surprisingly soluble in cold aromatic solvents, while *tert*-butyl dirotor, **1b**, was only highly soluble in acetone. *n*-Butyl and methoxy dirotors **1c** and **1d** were highly soluble. Compound **1c** formed a glassy solid from most solvents and a powder from dichloromethane/methanol. Dirotors with deuterated central phenylene rotators (**1a-d<sub>8</sub>–1d-d<sub>8</sub>**) for <sup>2</sup>H NMR studies were prepared by coupling 4-(3',3',3'-triphenylpropynyl)-1-bromobenzene- $d_4$ ,<sup>32</sup> **4-d<sub>4</sub>**, with the appropriate dialkynes.

The dirotors and their precursors were characterized by FTIR, <sup>1</sup>H NMR, <sup>13</sup>C NMR, and powder XRD. <sup>1</sup>H and <sup>13</sup>C NMR spectra of the dirotors **1a–1d** were consistent with a dynamically averaged structure reflecting symmetry about the *meta*-phenylene group that bridges the two rotators. The aromatic region of each dirotor has multiple signals due to the non-equivalent nature of the terminal trityl groups and the bridging bis(bistrityl) structure at the center of the structure. The 1,4-substituted aromatic ring of the rotator gave a signal corresponding to the expected AB pattern, which are shifted upfield from the rest of the signals of the trityl groups. The alkynyl and  $sp^3$  carbons on each side of the rotator are not chemically equivalent, giving resolvable signals in the <sup>13</sup>C NMR spectrum. The deuterated dirotors (**1a-d<sub>8</sub>–1d-d<sub>8</sub>**) have identical NMR spectra to their natural abundance counterparts, with the exception of the rotator signals, which are very small or absent due to lack of an internal NOE and the splitting due to coupling with the <sup>2</sup>H nucleus.

A detailed description of the local environment of each rotator requires analysis of the molecular and packing structures. While methoxy dirotor **1d** showed the greatest promise, diffraction quality single crystals would not be formed for any of the four derivatives. Examination of the X-ray powder diffraction patterns of **1a**, **1b**, and **1d** showed that powders formed by evaporation of solvent are indeed crystalline. The unsubstituted dirotor **1a**, the *tert*-butyl dirotor **1b**, and the methoxy dirotor **1d** have relatively sharp signals up to  $2\theta$  values of 25–30°, overlaying a broad featureless component at  $2\theta \approx 20$ , which suggests the presence of

Scheme 1. Synthesis of molecular dirotor compounds **1a–1d**.

small crystallites with an amorphous component. The *n*-butyl dirotor **1c** shows only a featureless pattern consistent with an amorphous solid.

## 2.2. Thermal analysis

Differential scanning calorimetry (DSC) and thermogravimetric analyses (TGA) were carried out with the same powder samples, which were used for dynamic studies using NMR spectroscopy (vide infra). As summarized in Table 1, endothermic peaks consistent with a melting transition were observed for compounds **1a**, **1b**, and **1d** in both natural abundance and deuterated forms. These were relatively broad, in agreement with the powder diffractogram, which had previously suggested a non-uniform sample phase. Samples of the *n*-butyl dirotor **1c** showed no melting transitions, which is consistent with visual observations of an opaque powder slowly softening and becoming increasingly translucent over a broad temperature range. The onset of decomposition for all eight dirotor samples occurred in the range of 350–430 °C, which is

essentially the same as that previously observed for the analogous molecular gyroscopes (370 °C).<sup>33</sup>

## 2.3. Solid-state <sup>13</sup>C CPMAS and NQS NMR spectroscopies

Line-shape changes occurring as a function of temperature in the <sup>13</sup>C CPMAS spectra can be used to measure exchange processes associated with rotary dynamics of phenylene groups in the kilo hertz regime.<sup>34–36</sup> The method takes advantage of the magnetic non-equivalence that exists in the solid state for phenylene nuclei that are related by an 180° rotation along the dialkyne axis. With a dynamic range that depends on the difference between their resonance frequencies, two signals are observed at lower temperatures when the exchange is slow. Broadening and coalescence occur as the exchange rate ( $k_{ex}$ ) approaches and supersedes the difference in resonance frequencies in hertz ( $\Delta\nu$ ),  $k_{ex} \geq 2\pi\delta\nu$ , until a single peak is observed in the fast exchange regime. Exploratory analysis of the <sup>13</sup>C CPMAS spectra revealed a complex aromatic region for all four dirotors. This is illustrated by the spectrum of unsubstituted dirotor **1a** in Figure 4. From the 14 non-equivalent aromatic signals distinguishable in solution, only two overlapping groups are observed between 140–150 ppm and 130–120 ppm in the solid state. The lack of resolution for the signals corresponding to rotator makes it impossible to use VT <sup>13</sup>C NMR spectroscopy as a dynamic characterization method. While we have shown that a strategy based on the deuteration of all the stator signals could make it possible, we decided to explore the use of <sup>2</sup>H NMR spectroscopy on samples where only the rotator is deuterated.

## 2.4. Rotational dynamics by quadrupolar <sup>2</sup>H NMR spectroscopy

Quadrupolar echo <sup>2</sup>H NMR spectroscopy is a well-defined powerful tool used to determine internal molecular dynamics in

**Table 1**  
Melting point and decomposition temperatures for dirotor compounds

Compound	Mp (°C)	Decomp. (°C)
<b>1a</b> (–H)	273–286	420
<b>1b</b> (– <i>t</i> -Bu)	221–234	430
<b>1c</b> (– <i>n</i> -Bu)	— <sup>a</sup>	395
<b>1d</b> (–OMe)	220–239	410
<b>1a-d<sub>8</sub></b> (–H)	279–289	430
<b>1b-d<sub>8</sub></b> (– <i>t</i> -Bu)	214–224	390
<b>1c-d<sub>8</sub></b> (– <i>n</i> -Bu)	— <sup>a</sup>	350
<b>1d-d<sub>8</sub></b> (–OMe)	225–240	410

<sup>a</sup> DSC shows no sharp melting point, consistent with the visual softening and liquifying over a large temperature range.

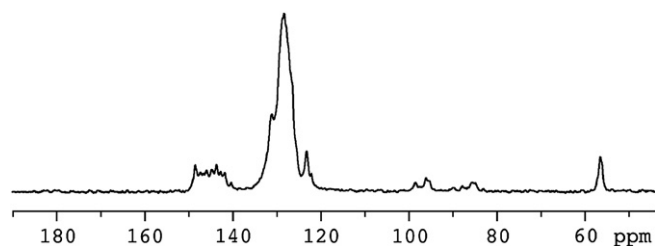


Figure 4.  $^{13}\text{C}$  CPMAS spectrum of dirotor **1a**.

the solid state.<sup>37–39</sup> As deuterium NMR spectroscopy is largely dominated by the orientation-dependent interaction between the nuclear spin and electric quadrupole moment at the nucleus, the characteristically broad spectrum from molecules in static powdered samples is strongly affected by internal molecular motions in the solid state. A single crystal with only one type of  $\text{C}^2\text{H}$  bond would give a doublet with a quadrupolar splitting  $\Delta\nu$  that depends on the orientation angle  $\beta$  that the bond makes with respect to the external field.<sup>40</sup>

$$\Delta\nu = 3/4(e^2q_{zz}Q/h)(3\cos^2\beta - 1) = 3/4\text{QCC}(3\cos^2\beta - 1)$$

$Q$  represents the electric quadrupole moment of the deuteron,  $e$  and  $h$  are the electric charge and Planck constant, and  $q_{zz}$  is the magnitude of the principal component of electric field gradient tensor, which lies along the  $\text{C}^2\text{H}$  bond. The frequency difference for signals of aromatic  $\text{C}^2\text{H}$  bonds, which have a  $\text{QCC} \approx 180$  kHz, changes from 135 kHz when  $\beta=0^\circ$  and 67.6 kHz for  $\beta=90^\circ$ , to 0 kHz when the  $\text{C}^2\text{H}$  bond is oriented at the magic angle of  $\beta=54.7^\circ$ . A collection of doublets in all possible orientations gives rise to a broad symmetric spectrum with two maxima and two shoulders known as a Pake or powder pattern. Variations in the powder pattern of a solid sample occur when the  $\text{C}^2\text{H}$  bonds experience reorientations, and line-shape analysis of the deuterium NMR spectra allows for the characterization of the type of motion, in terms of discrete jumps between different sites or continuous rotation, and for the determination of exchange rates in a range of ca.  $10^3$  to  $10^8$   $\text{s}^{-1}$ .

For our studies, we have taken advantage of the well characterized spectral changes occurring upon rotation of a phenylene group about its 1,4-axis.<sup>41–43</sup> Figure 5 illustrates spectral

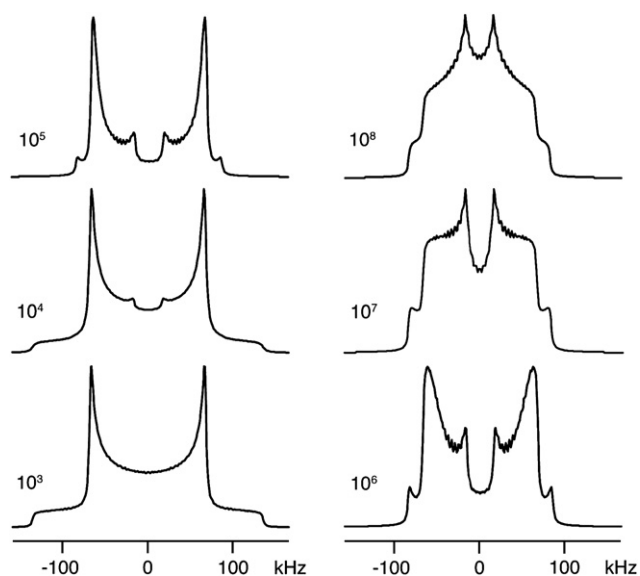


Figure 5. Simulated spectra for a dynamic process involving  $180^\circ$  jumps of a *para*-phenylene with exchange rates in hertz indicated on the left of each spectrum.

simulations using the program described by Nishikiori et al.<sup>44</sup> assuming a two-fold ( $180^\circ$ ) flipping model with a quadrupolar-coupling constant (QCC) of 180 kHz representative of the slow ( $k \leq 10^3$   $\text{s}^{-1}$ ), intermediate ( $10^4 \leq k \leq 10^7$   $\text{s}^{-1}$ ), and fast exchange regimes ( $k \geq 10^8$   $\text{s}^{-1}$ ).

Measurements with compounds **1a-d**<sub>8</sub>–**1d-d**<sub>8</sub> were carried out with a quadrupolar echo sequence on static powdered samples. Spectra were obtained at 46.07 MHz with  $90^\circ$  pulse width of 2.5  $\mu\text{s}$ , echo and refocusing delays of 35 and 25  $\mu\text{s}$ , respectively, and a delay of 5–10 s between pulses. The spectra acquired in the temperature range between 162 and 298 K are illustrated in Figure 6 with a line broadening function of 3 kHz. In spite of the different substituents and the varying degrees of crystallinity determined by XRPD, all four compounds gave qualitatively similar spectra with features characteristic of structurally heterogeneous samples. The lower temperature spectra (162–208 K) are consistent with exchange processes involving sites in the intermediate and fast regimes. Measurements between 231 and 243 K resulted in spectral data characteristic the fast exchange regime. And finally, the 298 K spectra for the substituted dirotors were significantly narrower than that expected for a dynamic process involving only two sites related by  $180^\circ$  rotation.

While the spectra derived from structurally complex samples are often comparable to the sum of spectra representing environments in the slow, intermediate, and fast components, a rigorous characterization in terms of a discrete number or a wide distribution of sites is very difficult.<sup>45</sup> Complexities arise not only from ambiguities in the number and type of spectral components, but also from the fact that their individual intensities depend both on their mole fraction and on their spin lattice relaxation times. Aware of these challenges, we decided to carry out simple simulations with the unique purpose of determining (a) whether or not a two-fold flipping process reasonably represents the data, and (b) the approximate regimes that best represent the rotary dynamics of the phenylene rotator.

As illustrated in the left column in Figure 7, the lower temperature spectra can be qualitatively simulated with components that experience two-fold flipping processes with exchange rates of  $10^5$  and  $10^8$   $\text{s}^{-1}$ . Symmetric sharp peaks at the edges and the center of the experimental spectrum, with a separation of 25 and 90 kHz, are consistent with those of the slower and faster components, respectively. The ambient temperature spectra have the inner peaks at 35 kHz, which are consistent with rotation of the phenylene along a relatively static axis, but the width of the spectrum is significantly narrower than that expected for a simple two-fold flipping process. It is well known that spectral narrowing occurs when the exchange process occurs with rotations involving more than two minima. Spectral simulations involving axially symmetric three-site or four-site processes with angular displacements of  $120^\circ$  or  $90^\circ$  in the fast exchange regime result in very narrow spectra with central peaks separated by a distance of 16 kHz, rather than the 25 kHz observed in our experiment.<sup>46</sup>

A qualitative model that accounts for our observations is based on contributions from two components in fast exchange (Fig. 7, right column). One component, involving a normal two-fold flipping process, accounts for the width in the lower part of the spectrum and at the baseline. The second component accounts for the narrow width on the top of the spectrum and requires more than two sites. For our simulation, we used a model that involves four energy minima at  $0^\circ$ ,  $30^\circ$ ,  $180^\circ$ , and  $220^\circ$  (Fig. 7h), which may be viewed as a combination of two two-fold processes (Fig. 8). A physical interpretation of this model could be related to local fluctuations in the environment of a two typical two-fold site. We believe this model describes the phenomenon observed at room temperature.

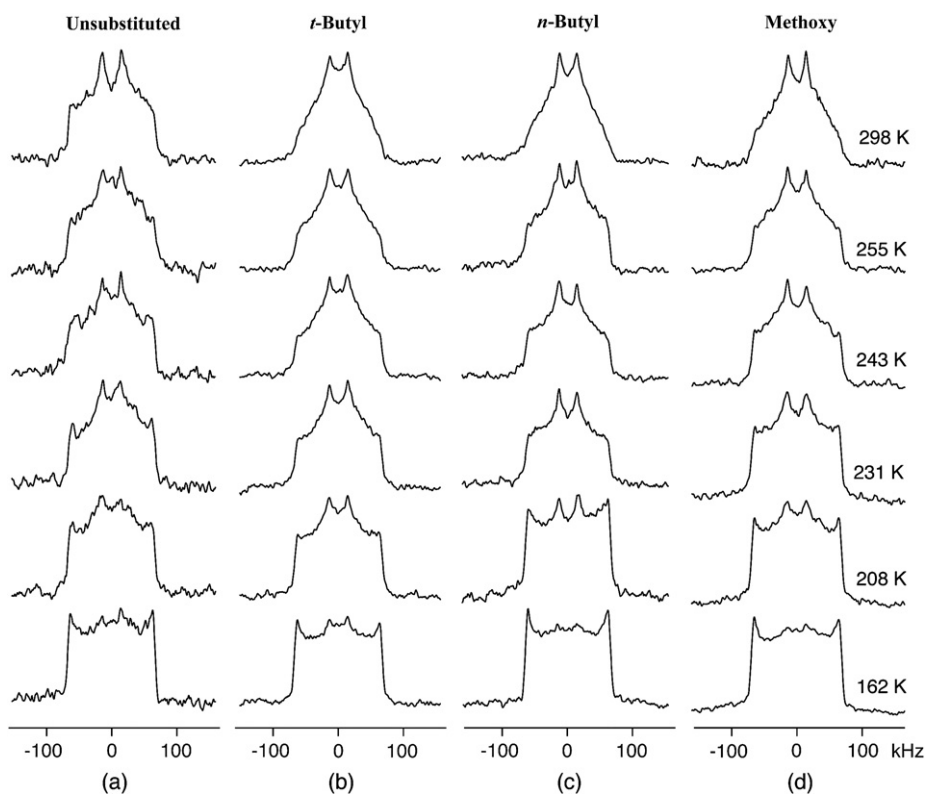


Figure 6. Experimental  $^2\text{H}$  NMR spectra for dirotors **1a-d<sub>8</sub>**–**1d-d<sub>8</sub>** acquired between 162 and 298 K.

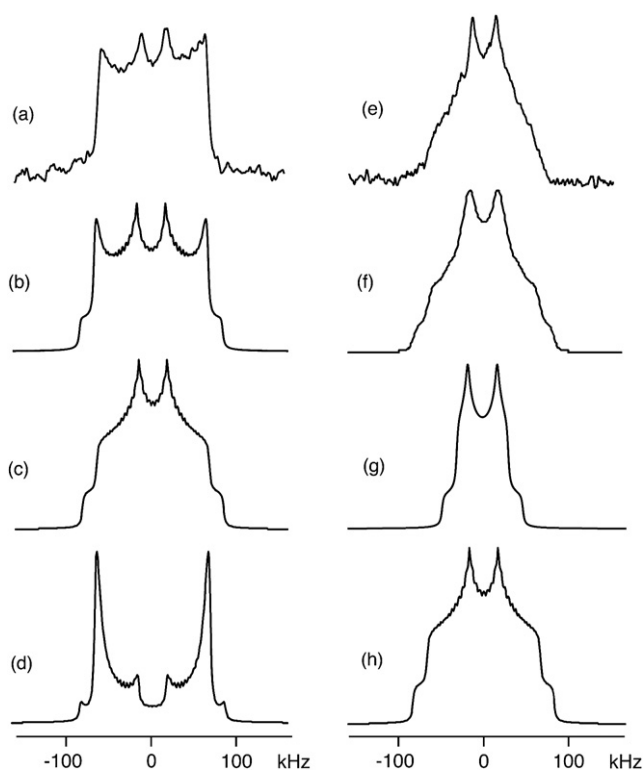


Figure 7. Quadrupolar echo  $^2\text{H}$  NMR spectra of dirotor **1c-d<sub>8</sub>** at 208 K: (a) experimental spectrum, (b) simulated spectrum as the sum of contributions of two-fold flipping models with exchange rates of (c)  $10^8$ , and (d)  $10^5 \text{ s}^{-1}$ .  $^2\text{H}$  NMR spectrum of dirotor **1c-d<sub>8</sub>** at 298 K: (e) experimental spectrum, (f) simulated spectrum as the sum of contributions with a two-fold flipping site with an exchange rate of (g)  $10^8$ , and (h) a four-site model with rotational minima at  $0^\circ$ ,  $30^\circ$ ,  $180^\circ$ , and  $220^\circ$  with exchange rates of  $10^8 \text{ s}^{-1}$ .

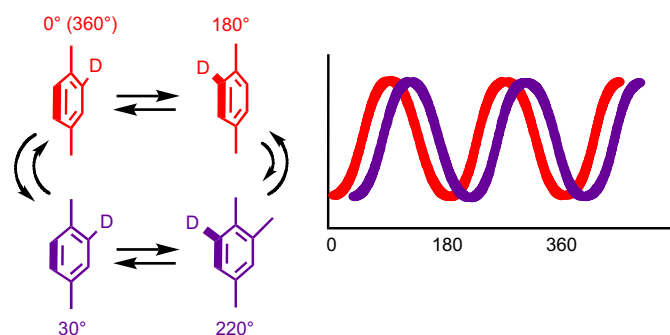


Figure 8. A hypothetical site exchange model involving two two-fold sites that are offset by  $30^\circ$ .

### 3. Conclusions

With four test samples, we have implemented a simple procedure for the synthesis of molecular dirotors of the wheel and axle types. As expected, challenges were found in the crystallization of these compounds, which tend to form finely powdered solids. X-ray diffraction and thermal analyses (DSC) data showed the structures of the parent compound (**1a**), the *tert*-butyl (**1b**), and the *para*-methoxy (**1d**) derivatives to be partially crystalline, and the structure of the *n*-butyl compound (**1c**) to be amorphous. While solid-state  $^{13}\text{C}$  CPMAS NMR measurements gave spectra with insufficient resolution for dynamic studies in the kilo hertz regime, quadrupolar echo  $^2\text{H}$  NMR spectra of phenylene-deuterated samples revealed a highly dynamic, if heterogeneous system. Spectral measurements between 162 and 230 K indicated sample domains with phenylene rotations varying from ca.  $10^4$  to  $10^8 \text{ s}^{-1}$ . Measurements at ca. 240 K were suggestive of rotations in the fast exchange regime, at  $\geq 10^8 \text{ s}^{-1}$ . Finally, ambient temperature spectra

were narrower than those expected for a two-fold flipping process in the fast exchange regime, but not narrow enough for continuous rotations. A simulated spectrum that accounts for the experimental one was based on a model that involves four sites, with two energy minima at 0° and 180° and two more at 30° and 220°. In conclusion, while these novel structures are clearly conducive to low-density materials that allow for fast internal dynamics, it will be desirable to find modifications that lead to crystalline materials. Studies with more rigid structures that prevent the reorientation of the two rotors and structures with photochemically active stators are currently in progress.

## 4. Experimental

### 4.1. General

The  $^1\text{H}$  and  $^{13}\text{C}$  NMR spectra were acquired on Bruker NMR spectrometer at 500 MHz and 125 MHz, respectively. Spectra were dissolved in  $\text{CDCl}_3$  or  $(\text{CD}_3)_2\text{CO}$  as indicated. Solid-state FTIR spectra were obtained on a PerkinElmer Spectrum 100 instrument. DSC and TGA analyses were recorded on PerkinElmer Pyris Diamond TG/DTA and DSC instruments. All reactions were run under inert atmosphere (argon). Mass spectrometry data was obtained with MALDI-TOF at the University of California, Riverside, Mass Spectrometry Center or at the University of California, Los Angeles, Molecular Instrumentation Center.

### 4.2. Materials

All reagent chemicals were purchased from Aldrich and used without further purification. All solvents were purchased from VWR. Reaction solvents were distilled prior to use. EMD Silica gel-60 (particle size 40–63 nm) purchased from VWR was used for column chromatography.

4-(3',3',3'-Triphenylpropynyl)-1-iodobenzene (**4**) and the deuterated equivalent 4-(3',3',3'-triphenylpropynyl)-1-bromobenzene- $d_4$  (**4-d<sub>4</sub>**) were prepared according to previously published procedures.<sup>32</sup>

#### 4.2.1. 1,3-Bis[1,1-diphenyl-1-hydroxymethyl]benzene (**2a**)

Lithium metal (0.63 g, 91 mmol) was stirred in 80 mL freshly distilled THF. After 20 min of stirring, 9.6 mL (91 mmol) bromobenzene was added. After 10 min, the dark brown solution was cooled to  $-78^\circ\text{C}$ . Dimethyl isophthalate (2.2 g, 11 mmol) was added. The solution was stirred for 48 h during which time the cold bath was allowed to naturally warm to room temperature. The reaction mixture was washed with satd aq  $\text{NH}_4\text{Cl}$  ( $\times 2$ ). The aqueous layer was extracted with  $\text{Et}_2\text{O}$  ( $\times 2$ ). The combined organic layers were dried with  $\text{Na}_2\text{SO}_4$  and concentrated. Purification was done with column chromatography (ethyl acetate/toluene; 2.5:97.5) to give 2.1 g (42% yield) of a white solid. Analysis: mp= $85\text{--}89^\circ\text{C}$ ;  $^1\text{H}$  NMR (500 MHz,  $\text{CDCl}_3$ ) 3.87 (s, 2H), 7.18–7.47 (m, 24H);  $^{13}\text{C}$  NMR (125 MHz,  $\text{CDCl}_3$ ) 81.76, 127.10, 127.67, 127.73, 127.88, 128.11, 131.66, 132.36; FTIR 3405 (br), 3057, 3025, 2950, 1953, 1896, 1812, 1700, 1614, 1597, 1490, 1446, 1312, 1277, 1205, 1159, 1140, 1112, 1094, 1022, 914, 891, 797, 756, 674, 696  $\text{cm}^{-1}$ . MS (MALDI-TOF) calculated for  $\text{C}_{32}\text{H}_{26}\text{O}_2$  442.2 [M] $^+$ ; found 425.2 [M–OH] $^+$ .

#### 4.2.2. 1,3-Bis[1,1-bis(4'-tert-butylphenyl)hydroxymethyl]benzene (**2b**)

Lithium metal (0.63 g, 91 mmol) was stirred in 200 mL freshly distilled THF. After 20 min, 16 mL (91 mmol) bromo-4-tert-butylbenzene was added. Upon the formation of the anion as indicated by a dark brown color the reaction mixture was cooled to  $-78^\circ\text{C}$  and 2.2 g (11 mmol) dimethyl isophthalate was added. The cold bath was allowed to warm naturally and the reaction mixture was

stirred for 48 h after which the reaction was quenched with saturated aqueous ammonium chloride. The aqueous layer was extracted with  $\text{Et}_2\text{O}$  ( $\times 3$ ). The combined organic layers were dried with  $\text{Na}_2\text{SO}_4$  and concentrated. Compound **2b** was purified by column chromatography (ethyl acetate/toluene; gradient of 0:1 to 1:20 by volume) to afford 3.2 g (42% yield) as a white solid. Analysis: mp= $174\text{--}176^\circ\text{C}$ ;  $^1\text{H}$  NMR (500 MHz,  $\text{CDCl}_3$ ) 1.29 (s, 36H), 7.08–7.42 (m, 20H);  $^{13}\text{C}$  NMR (125 MHz,  $\text{CDCl}_3$ ) 31.24, 34.32, 81.57, 124.57, 124.96, 126.27, 127.00, 127.47, 143.89, 146.46, 194.74; FTIR 3418 (br), 2959, 2903, 2867, 1724, 1662, 1604, 1508, 1475, 1460, 1401, 1362, 1269, 1201, 1171, 1108, 1017, 930, 894, 830, 796, 758, 715, 678  $\text{cm}^{-1}$ . MS (MALDI-TOF) calculated for  $\text{C}_{48}\text{H}_{58}\text{O}_2$  666.4 [M] $^+$ ; found 689.0 [M+Na] $^+$ .

#### 4.2.3. 1,3-Bis[1,1-bis(4'-n-butylphenyl)hydroxymethyl]benzene (**2c**)

Diol **2c** was synthesized following the same procedure described above for compound **2b** to give 3.0 g (39% yield) of a yellow oil.  $^1\text{H}$  NMR (500 MHz,  $\text{CDCl}_3$ ) 0.93 (t, 12H,  $J=7.5$  Hz), 1.35 (septet, 8H,  $J=7.5$  Hz), 1.55–1.61 (m, 8H), 2.36 (s, 2H), 2.58 (t, 8H,  $J=8$  Hz), 7.04 (d, 8H,  $J=6.5$  Hz), 7.09 (d, 8H,  $J=6.5$  Hz), 7.16–7.28 (m, 4H);  $^{13}\text{C}$  NMR (125 MHz,  $\text{CDCl}_3$ ) 13.85, 22.31, 33.43, 35.11, 81.70, 126.30, 127.65, 127.70, 128.12, 128.93, 141.57, 144.151, 146.53; FTIR 3454 (br) 3024, 2956, 2927, 2857, 1913, 1797, 1659, 1605, 1574, 1509, 1465, 1458, 1411, 1378, 1327, 1183, 1162, 1141, 1020, 2928, 891, 830, 795, 778, 729, 710, 695  $\text{cm}^{-1}$ . MS (MALDI-TOF) calculated for  $\text{C}_{48}\text{H}_{58}\text{O}_2$  667.0 [M] $^+$ ; found 649.0 [M–OH] $^+$  and 689.0 [M+Na] $^+$ .

#### 4.2.4. 1,3-Bis[1,1-bis(4'-methoxyphenyl)hydroxymethyl]benzene (**2d**)

Diol **2d** was obtained following a modified procedure similar to that of **2b**. Lithium metal (0.63 g, 91 mmol) was stirred in 100 mL THF at  $-78^\circ\text{C}$ . To the metal suspension, 12 mL (91 mmol) 4-bromoanisole was added. Stirring continued for 5 min then the cold bath was removed; formation of the anion as indicated by the dark color occurred within 20 min. The solution was cooled to  $-78^\circ\text{C}$  and 2.2 g (11 mmol) dimethyl isophthalate was added. The remaining procedure was same as for compound **2a**. Purification by column chromatography (methanol/dichloromethane; 1:99) afforded 4.7 g of a white solid (62% yield). Analysis: mp= $139\text{--}141^\circ\text{C}$ ;  $^1\text{H}$  NMR (500 MHz,  $\text{CDCl}_3$ ) 2.63 (s, 3H), 3.79 (s, 12H), 6.78 (d, 8H,  $J=10$  Hz), 7.10 (d, 8H,  $J=10$  Hz), 7.16–7.25 (m, 4H);  $^{13}\text{C}$  NMR (125 MHz,  $\text{CDCl}_3$ ) 55.18, 81.42, 113.00, 126.40, 127.29, 127.52, 129.04, 139.35, 146.86, 158.51; FTIR 3454 (br), 3024, 2956, 2927, 2857, 1913, 1797, 1659, 1605, 1574, 1509, 1483, 1465, 1458, 1411, 1378, 1327, 1183, 1162, 1141, 1020, 928, 891, 830, 795, 778, 729, 710, 695, 661  $\text{cm}^{-1}$ . MS (MALDI-TOF) calculated for  $\text{C}_{36}\text{H}_{34}\text{O}_6$  562.7 [M] $^+$ ; found 545.0 [M–OH] $^+$ .

#### 4.2.5. 1,3-Bis[1,1-diphenylprop-2-ynyl]benzene (**3a**)

Compound **2a** (1.5 g, 3.4 mmol) was refluxed in 20 mL acetyl chloride for 1 h. After cooling, excess acetyl chloride was removed by rotary evaporation. The white paste was dissolved in 10 mL dry benzene and rotary evaporated to remove all acetyl chloride twice. The residue was dissolved in 350 mL dry benzene and refluxed for 1 h. Ethynyl magnesium bromide (70 mL, 0.5 M in THF, 35 mmol) was added to the refluxing solution. Stirring continued at refluxing temperatures for 18 h. The cooled solution was quenched with satd aq  $\text{NH}_4\text{Cl}$ . The aqueous layer was extracted with  $\text{Et}_2\text{O}$  ( $\times 2$ ). The organic layers were combined and dried with  $\text{Na}_2\text{SO}_4$ . Purification of compound **3a** by column chromatography (toluene/hexanes; 30:20) resulted in 0.8 g (52% yield). Analysis: mp= $143\text{--}144^\circ\text{C}$ ;  $^1\text{H}$  NMR (500 MHz,  $\text{CDCl}_3$ ) 2.63 (s, 2H), 7.01–7.322 (m, 24H);  $^{13}\text{C}$  NMR (125 MHz,  $\text{CDCl}_3$ ) 44.42, 73.52, 89.38, 126.79, 127.17, 127.92, 128.22, 129.33, 130.51, 144.33, 144.62; FTIR 3305, 3283, 1596, 1490, 1445, 1420, 1261, 1182, 1156, 1099, 1032, 1002, 883, 797, 755, 660, 697  $\text{cm}^{-1}$ . MS (MALDI-TOF) calculated for  $\text{C}_{36}\text{H}_{25}$  457.2 [M–H] $^+$ ; found 457.2 [M–H] $^+$ .

#### 4.2.6. 1,3-Bis[1,1-bis(4'-tert-butylphenyl)prop-2-ynyl]benzene (**3b**)

Compound **3b** was synthesized following the same procedure as described above for compound **3a** using 1.2 g (1.8 mmol) **2b** to give 1.0 g (83% yield) of white solid. Analysis: mp=138–142 °C; <sup>1</sup>H NMR (500 MHz, CDCl<sub>3</sub>) 1.29 (s, 36H), 2.57 (s, 2H), 7.07 (d, 8H, *J*=8.5 Hz), 7.18–7.36 (m, 12H); <sup>13</sup>C NMR (125 MHz, CDCl<sub>3</sub>) 31.33, 34.35, 54.63, 73.06, 89.67, 124.71, 127.02, 127.33, 128.32, 128.52, 141.83, 144.40, 149.39; FTIR 3301, 2960, 2903, 2867, 1981, 1598, 1506, 1477, 1460, 1395, 1363, 1268, 1202, 1109, 1018, 925, 888, 827, 792, 753, 729, 713, 679 cm<sup>-1</sup>. MS (MALDI-TOF) calculated for C<sub>36</sub>H<sub>34</sub>O<sub>6</sub> 682.5; found 682.5.

#### 4.2.7. 1,3-Bis[1,1-bis(4'-n-butylphenyl)prop-2-ynyl]benzene (**3c**)

Compound **3c** was synthesized following the same procedure as described above for compound **3a** using 2.1 g (3.1 mmol) compound **2c** to give 1.3 g (62% yield) of yellow oil. <sup>1</sup>H NMR (500 MHz, CDCl<sub>3</sub>) 0.92 (t, 12H, *J*=7.5 Hz), 1.31–1.37 (m, 8H), 1.55–1.61 (m, 8H), 2.57 (t, 8H, *J*=8.0 Hz), 2.59 (s, 2H), 7.03 (d, 8H, *J*=8.5 Hz), 7.08 (d, 8H, *J*=8.5 Hz), 7.20–7.23 (m, 3H), 7.26 (s, 1H); <sup>13</sup>C NMR (125 MHz, CDCl<sub>3</sub>) 13.86, 22.30, 33.41, 35.05, 54.72, 73.05, 89.70, 127.09, 127.36, 127.75, 128.67, 130.43, 141.11, 142.01, 144.45; FTIR 3308, 3307, 3023, 2955, 2927, 2857, 1909, 1794, 1664, 1599, 1509, 1481, 1466, 1457, 1412, 1377, 1283, 1190, 1122, 1102, 1021, 929, 887, 829, 791, 777, 739, 706, 691 cm<sup>-1</sup>. MS (MALDI-TOF) calculated for C<sub>36</sub>H<sub>34</sub>O<sub>6</sub> 683.0 [M]<sup>+</sup>; found 705.0 [M+Na]<sup>+</sup>.

#### 4.2.8. 1,3-Bis[1,1-bis(4'-methoxybutylphenyl)prop-2-ynyl]benzene (**3d**)

Dialkyne **3d** was synthesized following the same procedure as described above for compound **3a** with a modification at the purification step. The reaction of 3.0 g (5.3 mmol) **2d** afforded 1.3 g of a white solid (41% yield) after purification by column chromatography (dichloromethane/hexane; 50:50). Analysis: mp=70–73 °C; <sup>1</sup>H NMR (500 MHz, CDCl<sub>3</sub>) 2.61 (s, 2H), 3.78 (s, 12H), 6.75 (d, 8H, *J*=9 Hz), 7.03–7.04 (m, 1H), 7.08 (d, 8H, *J*=9 Hz), 7.22–7.26 (m, 3H); <sup>13</sup>C NMR (125 MHz, CDCl<sub>3</sub>) 54.05, 55.20, 73.03, 89.85, 113.17, 127.29, 127.62, 129.93, 130.07, 137.11, 144.86, 158.24; FTIR 3283, 3001, 2954, 2932, 2904, 2835, 2548, 2051, 1892, 1676, 1606, 1582, 1506, 1481, 1461, 1440, 1422, 1297, 1246, 1175, 1116, 1031, 886, 825, 800, 737, 706, 689 cm<sup>-1</sup>. MS (MALDI-TOF) calculated for C<sub>40</sub>H<sub>34</sub>O<sub>4</sub> 578.3 [M]<sup>+</sup>; found 578.0 [M]<sup>+</sup>.

**4.2.8.1. Dirotor (1a).** Dialkyne, **3a** (0.15 g, 0.33 mmol), and 0.45 g (0.96 mmol) 4-(3',3',3'-triphenylpropynyl)-1-iodobenzene, **4**, were dissolved in 10 mL freshly distilled THF and 0.5 mL triethyl amine. The reaction mixture was degassed for 1 h prior to 98 mg (0.14 mmol) bis(triphenylphosphine)palladium dichloride and 53 mg (0.28 mmol) copper(II) iodide being added. The solution was stirred at 50 °C for 48 h. After cooling the solution was washed with satd aq NH<sub>4</sub>Cl. The organic layer was dried over Na<sub>2</sub>SO<sub>4</sub> and concentrated. The product was purified by column chromatography (benzene/hexanes; 30:70) to afford 90 mg (25% yield) of pure dirotor **1a** as a white solid. Analysis: mp=273–286 °C; <sup>1</sup>H NMR (500 MHz, CDCl<sub>3</sub>) 7.20–7.35 (m, 62H); <sup>13</sup>C NMR (125 MHz, CDCl<sub>3</sub>) 56.11, 56.15, 84.77, 84.95, 97.00, 97.29, 122.86, 126.78, 126.87, 127.43, 127.68, 127.98, 128.03, 129.01, 129.15, 130.66, 144.99, 145.19; FTIR 3056, 2956, 1726, 1740, 1696, 1490, 1446, 1263, 1182, 1157, 1103, 1079, 1032, 1002, 888, 837, 789, 756, 698 cm<sup>-1</sup>. MS (MALDI-TOF) calculated for C<sub>106</sub>H<sub>94</sub> 1366.74 [M]<sup>+</sup>; found 1367.7 [M]<sup>+</sup>.

**4.2.8.2. Dirotor (1b).** Dialkyne, **3b** (0.5 g, 0.7 mmol), and 1.0 g (2.1 mmol) 4-(3',3',3'-triphenylpropynyl)-1-iodobenzene, **4**, in 80 mL freshly distilled benzene and 1 mL diisopropylamine was degassed for 1 h with argon. Bis(triphenylphosphine)palladium dichloride (49 mg, 0.07 mmol) and 27 mg (0.14 mmol) copper(II) iodide were added and the solution refluxed for 48 h. After cooling the solution was quenched with saturated aqueous ammonium

chloride. The aqueous layer was extracted with Et<sub>2</sub>O (×3). The combined organic layers were dried with Na<sub>2</sub>SO<sub>4</sub> and concentrated. The product was purified by column chromatography (ethyl ether/hexanes; gradient of 0:1 to 1:49) to afford 0.5 g (50% yield) of a white solid. Analysis: mp=200–228 °C; <sup>1</sup>H NMR (500 MHz, (CD<sub>3</sub>)<sub>2</sub>CO) 1.26 (s, 36H), 7.20 (d, 8H, *J*=8.5 Hz), 7.26–7.36 (m, 42H), 7.45 (d, 4H, *J*=8.5 Hz), 7.52 (d, 4H, *J*=8.5 Hz); <sup>13</sup>C NMR (125 MHz, CDCl<sub>3</sub>) 30.61, 33.93, 55.25, 56.02, 84.79, 84.86, 97.16, 97.23, 122.96, 123.14, 124.75, 126.75, 126.87, 127.49, 127.98, 128.41, 128.83, 131.05, 131.40, 141.91, 145.00, 145.15, 149.42; FTIR 3058, 2960, 2925, 2854, 1734, 1596, 1490, 1462, 1445, 1363, 1261, 1180, 1156, 1079, 1032, 907, 840, 800, 772, 754, 733, 719, 696, 659 cm<sup>-1</sup>. MS (MALDI-TOF) calculated for C<sub>106</sub>H<sub>94</sub> 1366.8 [M]<sup>+</sup>; found 1391.0 [M+Na]<sup>+</sup>.

**4.2.8.3. Dirotor (1c).** Molecular rotor **1c** was prepared following the same procedure as for compound **1b** using 0.65 g (0.95 mmol) compound **3c**, 1.2 g (2.6 mmol) 4-(3',3',3'-triphenylpropynyl)-1-iodobenzene, **4**, 67 mg (0.095 mmol) bis(triphenylphosphine)palladium dichloride and 39 mg (0.19 mmol) copper iodide in 80 mL freshly distilled benzene and 1 mL diisopropylamine. Compound **1c** was obtained in 50% yield (0.65 g) as a glassy solid. <sup>1</sup>H NMR (500 MHz, (CD<sub>3</sub>)<sub>2</sub>CO) 0.84 (t, 12H, *J*=5 Hz), 1.25–1.32 (m, 8H), 1.48–1.56 (m, 8H), 2.55 (t, 8H, *J*=5 Hz), 7.09 (d, 8H, *J*=10 Hz), 7.15 (d, 8H, *J*=10 Hz), 7.25–35 (m, 34H), 7.41 (d, 4H, *J*=8.5 Hz), 7.51 (d, 4H, *J*=8.5 Hz); <sup>13</sup>C NMR (125 MHz, (CD<sub>3</sub>)<sub>2</sub>CO) 13.23, 22.05, 33.33, 34.70, 55.42, 56.02, 84.65, 84.77, 97.14, 97.33, 122.91, 123.13, 126.86, 127.88, 127.98, 128.64, 128.84, 130.71, 130.75, 131.34, 131.41, 132.28, 141.25, 142.21, 145.00, 145.31; FTIR cm<sup>-1</sup>. MS (MALDI-TOF) calculated for C<sub>106</sub>H<sub>94</sub> 1366.8 [M]<sup>+</sup>; found 1366.7 [M]<sup>+</sup>.

**4.2.8.4. Dirotor (1d).** Molecular rotor **1d** was prepared following the same procedure as for compound **1b** using 1.2 g (2.1 mmol) compound **3d**, 2.5 g (5.3 mmol) 4-(3',3',3'-triphenylpropynyl)-1-iodobenzene, **4**, 150 mg (0.21 mmol) bis(triphenylphosphine)palladium dichloride, and 800 mg (0.42 mmol) copper iodide in 80 mL freshly distilled benzene and 2 mL diisopropylamine. Compound **1d** was obtained in 69% yield (1.8 g) as a white solid. Analysis: mp=220–239 °C; <sup>1</sup>H NMR (500 MHz, (CD<sub>3</sub>)<sub>2</sub>CO) 3.73 (s, 12H), 6.82 (d, 8H, *J*=10 Hz), 7.14 (d, 8H, *J*=10 Hz), 7.19–7.40 (m, 34H), 7.51 (d, 4H, *J*=8.5 Hz); <sup>13</sup>C NMR (125 MHz, CDCl<sub>3</sub>) 54.79, 55.19, 56.18, 84.61, 84.91, 97.20, 97.50, 113.24, 122.97, 123.23, 126.89, 127.27, 127.59, 128.07, 129.17, 130.05, 130.37, 131.44, 131.50, 137.42, 145.23, 145.55, 158.24; FTIR cm<sup>-1</sup>. MS (MALDI-TOF) calculated for C<sub>94</sub>H<sub>70</sub>O<sub>4</sub> 1262.5 [M]<sup>+</sup>; found 1262.5 [M]<sup>+</sup>.

**4.2.8.5. Dirotor (1a-d<sub>8</sub>).** Dialkyne, **3a** (0.8 g, 1.7 mmol), and 2.2 g (5.2 mmol) 4-(3',3',3'-triphenylpropynyl)-1-bromobenzene-*d*<sub>4</sub>, **4-d<sub>4</sub>**, were dissolved in 10 mL freshly distilled THF and 10 mL diisopropylamine. The reaction mixture was degassed for 1 h prior to 240 mg (0.34 mmol) bis(triphenylphosphine)palladium dichloride and 130 mg (0.68 mmol) copper(II) iodide being added. The solution was stirred at 50 °C for 5 days. After cooling the solution was washed with satd aq NH<sub>4</sub>Cl. The organic layer was dried over Na<sub>2</sub>SO<sub>4</sub> and concentrated. Dirotor **1a-d<sub>8</sub>** was purified by column chromatography (benzene/hexanes; 30:70) to afford 90 mg (25% yield) of a white solid. Analysis: mp=279–289 °C; <sup>1</sup>H NMR (500 MHz, (CD<sub>3</sub>)<sub>2</sub>CO) 7.20–7.35 (m, 58H); <sup>13</sup>C NMR (125 MHz, CDCl<sub>3</sub>) 56.11, 56.15, 84.77, 84.95, 97.00, 97.29, 122.86, 126.78, 126.87, 127.43, 127.68, 127.98, 128.03, 129.01, 129.15, 130.66, 144.99, 145.19; FTIR 3056, 3032, 1597, 1490, 1446, 1424, 1321, 1182, 1157, 1080, 1033, 1002, 890, 853, 821, 786, 761, 756, 744, 728, 698 cm<sup>-1</sup>. MS (MALDI-TOF) calculated for C<sub>90</sub>H<sub>54</sub>D<sub>8</sub> 1150.54 [M]<sup>+</sup>; found 1173.5 [M+Na]<sup>+</sup>.

**4.2.8.6. Dirotor (1b-d<sub>8</sub>).** Dialkyne, **3b** (0.38 g, 0.56 mmol), and 0.60 g (1.4 mmol) 4-(3',3',3'-triphenylpropynyl)-1-bromobenzene-*d*<sub>4</sub>, **4-d<sub>4</sub>**, were dissolved in 25 mL freshly distilled THF and 1 mL

triethyl amine. The reaction mixture was degassed for 1 h. Bis-(triphenylphosphine)palladium dichloride (77 mg, 0.11 mmol) and 43 mg (0.22 mmol) copper(II) iodide being added. The solution was stirred at 50 °C for 48 h. After cooling the solution was washed with satd aq NH<sub>4</sub>Cl. The organic layer was dried over Na<sub>2</sub>SO<sub>4</sub> and concentrated. Dirotor **1b-d<sub>8</sub>** was purified by column chromatography (dichloromethane/hexanes; 30:70) to afford 90 mg (25% yield) of a white solid. Analysis: mp=268–272 °C; <sup>1</sup>H NMR (500 MHz, (CD<sub>3</sub>)<sub>2</sub>CO) 1.25 (s, 36H), 7.01–7.34 (m, 50H); <sup>13</sup>C NMR (125 MHz, (CD<sub>3</sub>)<sub>2</sub>CO) 30.59, 33.94, 55.36, 56.05, 84.21, 84.64, 96.98, 97.25, 124.76, 124.89, 126.81, 127.93, 128.26, 128.35, 128.83, 141.90, 144.99, 149.45, 149.70; FTIR 3058, 2959, 2902, 2865, 1598, 1505, 1491, 1460, 1447, 1423, 1394, 1363, 1268, 1185, 1109, 1018, 889, 827, 792, 755, 727, 712, 697, 675, 660 cm<sup>-1</sup>. MS (MALDI-TOF) calculated for C<sub>106</sub>H<sub>86</sub>D<sub>8</sub> 1374.78 [M]<sup>+</sup>; found 1374.8 [M]<sup>+</sup>.

4.2.8.7. Dirotor (**1c-d<sub>8</sub>**). Dialkyne, **3c** (0.36 g, 0.53 mmol), and 0.50 g (1.2 mmol) 4-(3',3',3'-triphenylpropynyl)-1-bromobenzene-**d<sub>4</sub>**, **4-d<sub>4</sub>**, were dissolved in 30 mL freshly distilled THF and 1 mL triethyl amine. Following degassing for 1 h, 35 mg (0.05 mmol) bis(triphenylphosphine)palladium dichloride and 19 mg (0.10 mmol) copper(II) iodide were added. The solution was stirred at 50 °C for 48 h. After cooling the solution was washed with satd aq NH<sub>4</sub>Cl. The organic layer was dried over Na<sub>2</sub>SO<sub>4</sub> and concentrated. Dirotor **1c-d<sub>8</sub>** was purified by column chromatography (dichloromethane/hexanes; 10:90) to afford 330 mg (46% yield) of a glassy solid. <sup>1</sup>H NMR (500 MHz, CDCl<sub>3</sub>) 0.87–0.92 (m, 12H), 1.26–1.38 (m, 8H), 1.52–1.59 (m, 8H), 2.46–2.57 (m, 8H), 6.93–7.31 (m, 50H); <sup>13</sup>C NMR (125 MHz, CDCl<sub>3</sub>) 13.96, 22.42, 33.46, 35.14, 55.42, 56.02, 84.65, 84.77, 97.14, 97.33, 126.84, 126.87, 127.88, 128.01, 128.74, 128.84, 129.15, 141.15, 141.21, 141.71, 142.46, 145.18; FTIR 3084, 3057, 3054, 2955, 2827, 2857, 1947.6, 1904, 1800, 1597, 1508, 1491, 1465, 1447, 1424, 1377, 1322, 1296, 1249, 1186, 1121, 1102, 1080, 1034, 1020, 1002, 965, 929, 887, 853, 828, 777, 756, 727, 697, 658 cm<sup>-1</sup>. MS (MALDI-TOF) calculated for C<sub>106</sub>H<sub>86</sub>D<sub>8</sub> 1374.78 [M]<sup>+</sup>; found 1374.8 [M]<sup>+</sup>.

4.2.8.8. Dirotor (**1d-d<sub>8</sub>**). Dialkyne, **3d** (0.36 g, 0.60 mmol), and 0.78 g (1.8 mmol) 4-(3',3',3'-triphenylpropynyl)-1-bromobenzene-**d<sub>4</sub>**, **4-d<sub>4</sub>**, were dissolved in 23 mL freshly distilled benzene and 1 mL triethyl amine and then degassed for 1 h followed by the addition of 42 mg (0.06 mmol) bis(triphenylphosphine)palladium dichloride and 23 mg (0.12 mmol) copper(II) iodide. The solution was refluxed for 48 h. After cooling the solution was washed with satd aq NH<sub>4</sub>Cl. The organic layer was dried over Na<sub>2</sub>SO<sub>4</sub> and concentrated. Dirotor **1d-d<sub>8</sub>** was purified by column chromatography (dichloromethane/hexanes; 40:60) to afford 180 mg (23% yield) of a white solid. Analysis: mp=225–240 °C; <sup>1</sup>H NMR (500 MHz, (CD<sub>3</sub>)<sub>2</sub>CO); 3.75 (s, 12H), 6.83 (d, 8H, J=9 Hz), 7.14 (d, 8H, J=9 Hz), 7.20–7.41 (m, 34H); <sup>13</sup>C NMR (125 MHz, CDCl<sub>3</sub>) 54.78, 55.16, 56.15, 84.85, 85.01, 97.24, 97.55, 113.22, 122.76, 122.99, 126.88, 127.20, 127.60, 128.03, 129.15, 130.03, 137.45, 145.19, 145.54, 158.21; FTIR 3057, 2931, 2833, 1605, 1582, 1507, 1490, 1461, 1447, 1424, 1297, 1248, 1176, 1114, 1034, 889, 828, 800, 784, 755, 727, 698, 655 cm<sup>-1</sup>. MS (MALDI-TOF) calculated for C<sub>94</sub>H<sub>62</sub>D<sub>8</sub>O<sub>4</sub> 1270.58 [M]<sup>+</sup>; found 1270.6 [M]<sup>+</sup>.

## Acknowledgements

We would like to thank NSF grant DMR0605688. S.L.G. and R.B.R. were supported by NSF discovery corps grant CHE0513503.

## Supplementary data

Supplementary data associated with this article can be found in the online version, at doi:10.1016/j.tet.2008.05.143.

## References and notes

- (a) Kay, E. R.; Leigh, D. A.; Zerbetto, F. *Angew. Chem., Int. Ed.* **2007**, *46*, 72–191; (b) Marsella, M. J.; Rahbarnia, S.; Wilmont, N. *Org. Biomol. Chem.* **2007**, *5*, 391–400; (c) Skopek, K.; Hershberger, M. C.; Gladysz, J. A. *Coord. Chem. Rev.* **2007**, *251*, 1723–1733; (d) Shirai, Y.; Morin, J.-F.; Sasaki, T.; Guerrero, J. M.; Tour, J. M. *Chem. Soc. Rev.* **2006**, *35*, 1043–1055; (e) Kottas, G. S.; Clarke, L. I.; Horinek, D.; Michl. *Chem. Rev.* **2005**, *105*, 1281–1376; (f) Balzani, V.; Margherita, V.; Credi, A. *Molecular Devices and Machines*; Wiley-VCH: Weinheim, 2003; (g) Feringa, B. L.; Koumura, N.; Delden, R. A.; TerWiel, M. K. *Appl. Phys. A* **2002**, *75*, 301–308; (h) Sestelo, J. P.; Kelly, T. R. *Appl. Phys. A* **2002**, *75*, 337–343; (i) Balzani, V.; Credi, A.; Raymo, F.; Stoddart, J. *Angew. Chem., Int. Ed.* **2000**, *39*, 3349–3391.
- (a) Stoddart, J. F. *Acc. Chem. Res.* **2001**, *34*, 433–444; (b) Saha, S.; Flood, A. H.; Stoddart, J. F.; Impellizzeri, S.; Silvi, S.; Venturi, M.; Credi, A. *J. Am. Chem. Soc.* **2007**, *129*, 12159–12171; (c) Nygaard, S.; Laursen, B. W.; Flood, A. M.; Hansen, N. C.; Jeppesen, J. O.; Stoddart, J. F. *Chem. Commun.* **2006**, 144–146.
- (a) Feringa, B. L. *J. Org. Chem.* **2007**, *72*, 6635–6652; (b) Vicario, J.; Walko, M.; Meetsma, A.; Feringa, B. L. *J. Am. Chem. Soc.* **2006**, *128*, 5127–5135; (c) Vicario, J.; Katsonis, N.; Ramon, B. S.; Bastiaansen, C. W. M.; Broer, D. J.; Feringa, B. L. *Nature* **2006**, *440*, 163; (d) ter Wiel, M. K. J.; van Delden, R. A.; Meetsma, A.; Feringa, B. L. *J. Am. Chem. Soc.* **2005**, *127*, 14208–14222; (e) Fletcher, S. P.; Dumur, F.; Pollard, M. M.; Feringa, B. L. *Science* **2005**, *310*, 80–82.
- (a) Horinek, D.; Michl, J. *Proc. Natl. Acad. Sci. U.S.A.* **2005**, *102*, 14175–14180; (b) Vacek, J.; Michl, J. *Adv. Funct. Mater.* **2007**, *17*, 730–739; (c) Zheng, X.; Mulcahy, M. E.; Horinek, D.; Galeotti, F.; Magnera, T.; Michl, J. *J. Am. Chem. Soc.* **2004**, *126*, 4540–4542; (d) Balzani, V.; Credi, A.; Venturi, M. *Chem. Phys. Chem.* **2008**, *9*, 202–220.
- (a) Shirai, Y.; Osgood, A. J.; Zhao, Y.; Yao, Y.; Saudan, L.; Yang, H.; Yu-Hung, C.; Alemany, L. B.; Sasaki, T.; Morin, J. F.; Guerrero, J. M.; Kelly, K. F.; Tour, J. M. *J. Am. Chem. Soc.* **2006**, *128*, 4854–4864; (b) Sasaki, T.; Osgood, A. J.; Alemany, L. B.; Kelly, K. F.; Tour, J. M. *Org. Lett.* **2008**, *10*, 229–232.
- (a) Nguyen, T. D.; Liu, Y.; Saha, S.; Leung, K. C. F.; Stoddart, J. F.; Zink, J. I. *J. Am. Chem. Soc.* **2007**, *129*, 626–634; (b) Nguyen, T. D.; Leung, K. C.-F.; Liong, M.; Liu, Y.; Stoddart, J. F.; Zink, J. I. *Adv. Funct. Mater.* **2007**, *17*, 2101–2110; (c) Aprahamian, I.; Yasuda, T.; Ikeda, T.; Saha, S.; Dichtel, W. R.; Isoda, K.; Kato, T.; Stoddart, J. F. *Angew. Chem., Int. Ed.* **2007**, *119*, 4759–4763; (d) Liu, Y.; Flood, A. H.; Bonvallet, P. A.; Vignon, S. A.; Northrop, B.; Tseng, H.-R.; Jeppesen, J.; Huang, T. J.; Brough, B.; Baller, M.; Magonov, S.; Solares, S.; Goddard, W. A., III; Ho, C.-M.; Stoddart, J. F. *J. Am. Chem. Soc.* **2005**, *127*, 9745–9759; (e) Nguyen, T.; Tseng, H.-R.; Celestre, P. C.; Flood, A. H.; Liu, Y.; Zink, J. I.; Stoddart, J. F. *Proc. Natl. Acad. Sci. U.S.A.* **2005**, *102*, 10029–10034.
- Karlen, S. D.; Garcia-Garibay, M. A. *Top. Curr. Chem.* **2006**, *262*, 179–228.
- (a) Horike, S.; Matsuda, R.; Tanaka, D.; Matsubara, S.; Mizuno, M.; Endo, K.; Kitagawa, S. *Angew. Chem., Int. Ed.* **2006**, *43*, 7226–7230; (b) Sato, D.; Akutagawa, T.; Takeda, S.; Noro, S.; Nakamura, T. *Inorg. Chem.* **2007**, *46*, 363–365; (c) Sato, N.; Nishikiori, S. I. *Dalton Trans.* **2007**, 1115–1119; (d) Zhou, W.; Yildirim, T. *Phys. Rev. B* **2006**, *74*, 180301–1–180301-4.
- Sokolov, A. N.; Swenson, D. C.; MacGillivray, L. R. *Proc. Natl. Acad. Sci. U.S.A.* **2008**, *105*, 1794–1797.
- Garcia-Garibay, M. A. *Proc. Natl. Acad. Sci. U.S.A.* **2005**, *102*, 10771–10776.
- Khuong, T. A. V.; Nunez, J. E.; Godinez, C. E.; Garcia-Garibay, M. A. *Acc. Chem. Res.* **2006**, *39*, 413–422.
- Sipachev, V. A.; Khaikin, L. S.; Grikina, O. E.; Nikitin, V. S.; Traetteberg, M. *J. Mol. Struct.* **2000**, *523*, 1–22.
- Dominguez, Z.; Dang, H.; Strouse, M. J.; Garcia-Garibay, M. A. *J. Am. Chem. Soc.* **2002**, *124*, 2398–2399.
- Dominguez, Z.; Dang, H.; Strouse, J. M.; Garcia-Garibay, M. A. *J. Am. Chem. Soc.* **2002**, *124*, 7719–7727.
- Khuong, T. A. V.; Zepeda, G.; Ruiz, R.; Kahn, S. I.; Garcia-Garibay, M. A. *Cryst. Growth Des.* **2004**, *4*, 15–18.
- Godinez, C. E.; Zepeda, G.; Garcia-Garibay, M. A. *J. Am. Chem. Soc.* **2002**, *124*, 4701–4707.
- Khuong, T.-A. V.; Dang, H.; Jarowski, P. D.; Maverick, E. F.; Garcia-Garibay, M. A. *J. Am. Chem. Soc.* **2007**, *129*, 839–845.
- Jarowski, P. D.; Houk, K. N.; Garcia-Garibay, M. A. *J. Am. Chem. Soc.* **2007**, *129*, 3110–3117.
- Horansky, R. D.; Clarke, L. I.; Price, J. C.; Khuong, T.-A. V.; Jarowski, P. D.; Garcia-Garibay, M. A. *Phys. Rev. B* **2005**, *B72*, 014302–1–014302-5.
- Horansky, R. D.; Clarke, L. I.; Winston, E. B.; Price, J. C.; Karlen, S. D.; Jarowski, P. D.; Santillan, R.; Garcia-Garibay, M. A. *Phys. Rev. B* **2006**, *74*, 054306–1–054306-12.
- For a review on related structures see: McNicol, D. D.; Toda, F.; Bishop, R. *Comprehensive Supramolecular Chemistry*; Pergamon: Oxford, 1996; Vol. 6.
- Soldatov, D. V. *J. Chem. Crystallogr.* **2006**, *36*, 747–768.
- Toda, F.; Akagi, K. *Tetrahedron Lett.* **1968**, *9*, 3695–3698.
- Toda, F.; Ward, D. L.; Hart, H. *Tetrahedron Lett.* **1981**, *22*, 3865–3868.
- Hart, H.; Lin, L. T. W.; Ward, D. L. *J. Am. Chem. Soc.* **1984**, *106*, 4043–4045.
- Jetti, R. K. R.; Kuduva, S. S.; Reddy, D. S.; Xue, F.; Mak, T. C. W.; Nangia, A.; Desiraju, G. R. *Tetrahedron Lett.* **1998**, *39*, 913–916.
- Joachim, C.; Tang, H.; Moresco, F.; Rapenne, G.; Meyer, G. *Nanotechnology* **2002**, *13*, 330–335.
- Soldatov, D. V.; Moudrakovski, I. L.; Ratcliffe, C. I.; Dutrisac, R.; Ripmeester, J. A. *Chem. Mater.* **2003**, *15*, 4810–4818.
- Soldatov, D. V.; Tinnemans, P.; Enright, G. D.; Ratcliffe, C. I.; Diamante, P. R.; Ripmeester, J. A. *Chem. Mater.* **2003**, *15*, 3826–3840.
- Host-guest interactions have also been exploited to create low-density and/or solvent inclusion crystalline solids. For recent advances using this motif see: (a)

- Ashmore, J.; Bishop, R.; Craig, D. C.; Scudder, M. L. *Cryst. Growth Des.* **2007**, *7*, 47–55; (b) Rahman, A. N. M. M.; Bishop, R.; Craig, D. C.; Scudder, M. L. *Org. Biomol. Chem.* **2004**, *2*, 175–182; (c) Maly, K. E.; Gagnon, E.; Maris, T.; Wuest, J. D. *J. Am. Chem. Soc.* **2007**, *129*, 4306–4322; (d) Trolliet, C.; Poulet, G.; Tuel, A.; Wuest, J. D.; Sautet, P. *J. Am. Chem. Soc.* **2007**, *129*, 3621–3626.
31. Gould, S. L.; Tranchemontagne, D.; Yaghi, O. M.; Garcia-Garibay, M. A. *J. Am. Chem. Soc.* **2008**, *130*, 7707–7710.
32. Karlen, S. D.; Godinez, C. E.; Garcia-Garibay, M. A. *Org. Lett.* **2006**, *8*, 3417–3420.
33. Dominguez, Z.; Khuong, T. A. V.; Sanrame; Dang, H.; Garcia-Garibay, M. A. *J. Am. Chem. Soc.* **2003**, *125*, 8827–8837.
34. Karlen, S. D.; Garcia-Garibay, M. A. *Chem. Commun.* **2005**, 189–191.
35. Bain, A. D. *Prog. Nucl. Magn. Reson. Spectrosc.* **2003**, *43*, 63–103.
36. Riddell, F. G.; Cameron, K. S.; Holmes, S. A.; Strange, J. H. *J. Am. Chem. Soc.* **1997**, *119*, 7555–7560.
37. Sillescu, H. *Pure Appl. Chem.* **1982**, *54*, 619–626.
38. Spiess, H. W. *Colloid Polym. Sci.* **1983**, *261*, 193–209.
39. Hoatson, G. L.; Vold, R. L. *Solid-state NMR III*; Blümich, B., Ed.; Springer: New York, NY, 1994; pp 1–67.
40. This equation assumes negligible asymmetry in the electric field gradient tensor:  $\eta = (q_{xx} - q_{yy})/q_{zz} = 0$ . Deviations from this condition are generally small for aromatic deuterons.
41. Cholli, A. L.; Dumais, J. J.; Engel, A. K.; Jelinski, L. W. *Macromolecules* **1984**, *17*, 2399–2404.
42. Rice, D. M.; Witebort, R. J.; Griffin, R. G.; Meirovich, E.; Stimson, E. R.; Meinwald, Y. C.; Freed, J. H.; Scheraga, H. A. *J. Am. Chem. Soc.* **1981**, *103*, 7707–7710.
43. Rice, D. M.; Meinwald, Y. C.; Scheraga, H. A.; Griffin, R. G. *J. Am. Chem. Soc.* **1987**, *109*, 1636–1640.
44. Nishikiori, S. I.; Soma, T.; Iwamoto, T. *J. Inclusion Phenom. Mol. Recognit. Chem.* **1997**, *27*, 233–243.
45. Wehrle, M.; Hellmann, G. P.; Spiess, H. W. *Colloid Polym. Sci.* **1987**, *265*, 815–822.
46. For line-shape simulations involving two-fold (180°), three-fold (120°), and four-fold jumps, please see Supplementary data.